Long-lived biνo at the LHC

Julia Gehrlein[a] **and Seyda Ipek**[b]

[a] *High Energy Theory Group, Physics Department, Brookhaven National Laboratory,*
Upton, NY 11973, U.S.A.

[b] *Department of Physics and Astronomy, University of California,*
Irvine 4129 Frederick Reines Hall, Irvine, CA 92617-4575, U.S.A.

E-mail: jgehrlein@bnl.gov., sipek@uci.edu

ABSTRACT: We examine the detection prospects for a long-lived biνo, a pseudo-Dirac bino which is responsible for neutrino masses, at the LHC and at dedicated long-lived particle detectors. The biνo arises in $U(1)_R$-symmetric supersymmetric models where the neutrino masses are generated through higher dimensional operators in an inverse seesaw mechanism. At the LHC the biνo is produced through squark decays and it subsequently decays to quarks, charged leptons and missing energy via its mixing with the Standard Model neutrinos. We consider long-lived biνos which escape the ATLAS or CMS detectors as missing energy and decay to charged leptons inside the proposed long-lived particle detectors FASER, CODEX-b, and MATHUSLA. We find the currently allowed region in the squark-biνo mass parameter space by recasting most recent LHC searches for jets+$\not{E}_T$. We also determine the reach of MATHUSLA, CODEX-b and FASER. We find that a large region of parameter space involving squark masses, biνo mass and the messenger scale can be probed with MATHUSLA, ranging from biνo masses of $10\,\text{GeV-2}\,\text{TeV}$ and messenger scales $10^{2-11}\,\text{TeV}$ for a range of squark masses.

KEYWORDS: Beyond Standard Model, Neutrino Physics, Supersymmetric Standard Model

Contents

1 Introduction

There are several open questions in particle physics which cannot be answered by the Standard Model (SM). Amongst the most pressing ones are the generation of neutrino masses, the need for a dark matter candidate, and a mechanism to generate the observed baryon asymmetry of the universe. As searches for new physics particles in different environments have so far come up empty handed, novel search strategies need to be developed.

One possibility is to extend the searches to look for particles which do not decay promptly at particle colliders but have a macroscopic decay length. In the last several years large interest has arisen to search for long-lived particles (LLPs) as several detectors at the LHC have been proposed [1–9] and detailed investigations from the model building side have been done (see [10, 11] for recent reviews). Many minimal supersymmetric models (MSSM) naturally give rise to LLPs such that they can serve as benchmark models for various analyses. In most supersymmetric models the LLP is the next-to-lightest supersymmetric particle (NLSP) which decays into the lightest supersymmetric particle (LSP). But, for example, R-parity violating supersymmetry allows a final state which contains purely SM particles.

In this work we study the prospect of probing the parameter space of a certain R-symmetric MSSM model, introduced in [12] and studied in more detail in [13], via LLP searches. In R-symmetric MSSM the superpartners are charged under a global $U(1)_R$ symmetry while the SM particles are neutral [14]. Due to this global symmetry gauginos are expected to be Dirac fermions. However the global $U(1)_R$ is broken because the gravitino acquires a mass, which then leads to small $U(1)_R$-breaking Majorana masses for gauginos such that they are pseudo-Dirac fermions having both Dirac and Majorana masses [15–17].[1]

---

[1]To obtain Dirac masses for the gauginos additional adjoint fields with opposite $U(1)_R$ need to be introduced [18, 19]. See section 2.

The collider phenomenology of R-symmetric MSSM differs from the MSSM phenomenology. For example, some production channels for supersymmetric particles are not available due to the $U(1)_R$ symmetry. In general collider limits on R-symmetric MSSM tend to be less stringent than the ones on MSSM [13, 20–23].

In the model we study, the $U(1)_R$ symmetry is elevated to $U(1)_{R-L}$, where L is lepton number. It has been shown in [12] that the pseudo-Dirac bino, dubbed biνo, in this model can play the role of right-handed neutrinos and that light Majorana neutrino masses are generated via an inverse-seesaw mechanism. The smallness of the light neutrino masses is generated by a hierarchy between the source of $U(1)_R$ breaking, namely the gravitino mass $m_{3/2}$, and the messenger scale Λ_M. Furthermore, the decay rate of the biνo is inversely proportional to the messenger scale. Hence probing different possible lifetimes of the biνo provides valuable information on the messenger scale and the origin of neutrino masses in this model.

In [13] biνo decays at the LHC were investigated in order to find the constraints on squark and biνo masses. In that work the messenger scale was set to $\Lambda_M = 100$ TeV, a scale expected to be probed by low energy experiments like Mu2e, and only biνo masses $O(100 \text{ GeV})$ were investigated. At this scale the biνo decays promptly and the strongest constraints come from ATLAS jets+$\not{E}_T$ search, where the missing energy comes from neutrinos produced in biνo decays in contrast to the LSP as in most other MSSM models. As the messenger scale rises, biνo decay width becomes smaller, making the biνo long-lived at LHC scales. In this work we study the prospects of probing $\Lambda_M > 10^5$ TeV. At these scales biνo would be considered as missing energy in ATLAS and CMS jets+$\not{E}_T$ searches, while it can decay into charged leptons inside proposed LLP detectors like MATHUSLA, FASER and CODEX-b. To this aim we will contrast the constraints from jets+$\not{E}_T$ searches at the LHC with $\sqrt{s} = 13\,\text{TeV}$ and $\mathcal{L} = 36$ fb^{-1} with forecasted searches using the same channel with $\mathcal{L} = 3$ ab^{-1} at MATHUSLA, FASER and CODEX-b. We show that while FASER and its upgraded version FASER 2 are not competitive against jets+$\not{E}_T$ searches, MATHUSLA and CODEX-b can probe the messenger scale over a wide range of parameter space, $\Lambda_M \sim 10^{5-12}$ TeV for biνo and squark masses of $O(100 \text{ GeV} - \text{TeV})$. Our results are given in figure 4.

This manuscript is organized as follows: we give a brief overview of the model in section 2, in section 3 we provide analytical results for the biνo lifetime and decay length, section 4 is devoted to our numerical study of the bino phenomenology including the reach of LHC and LLP searches, and we summarize and conclude in section 5.

2 Model

The details of this model have been given in [12, 13]. In this section we briefly summarize the salient points important for our analysis.

The model we work with is a modified version of $U(1)_R$-symmetric MSSM, in which we impose a global $U(1)_{R-L}$ symmetry, where L is the lepton number, on the supersymmetric sector. SM particles are not charged under $U(1)_R$, but of course some of them have lepton charges. Employing the lepton number is essential to generating the interactions between

Superfields	$U(1)_R$	$U(1)_{R-L}$
L	1	0
E^c	1	2
$H_{u,d}$	0	0
$R_{u,d}$	2	2
$W_{\tilde{B}}$	1	1
Φ_S	0	0
gravitino/goldstini	1	1

Table 1. The relevant field content of the $U(1)_R$ symmetric model (SM charges not shown). L, E^c are the lepton superfields and $H_{u,d}$ are the up-type and down-type Higgs superfields. The fermionic components of the superfields $R_{u,d}$ are the Dirac partners of the Higgsinos $\tilde{h}_{u,d}$. Φ_S is a superfield which has the same SM charges as $W_{\tilde{B}}$ and its fermionic component S is the Dirac partner of the bino.

bino and the SM neutrinos. Some of the supersymmetric fields and their $U(1)_R, U(1)_{R-L}$ charges are given in table 1.

This model inherits many properties of $U(1)_R$-symmetric MSSM. The most prominent feature of these models is that gauginos are Dirac due the global $U(1)$ symmetry. As such, for each gaugino with $U(1)_R$ charge of 1, a Dirac partner is introduced with -1 R charge. Here we will only focus on the bino, $\tilde{B}$, and its Dirac partner the singlino, S.

Supersymmetry is broken in a hidden sector which communicates with the visible sector at a messenger scale Λ_M and is incorporated via $F-$ and D-term spurions, $X = \theta^2 F$ and $W'_\alpha = \theta_\alpha D$ respectively. The F-term generates masses for the sfermions while the D-term spurion generates the Dirac gaugino masses via the supersoft term [24]

$$\int d^2\theta \frac{\sqrt{2}c_i}{\Lambda_M} W'_\alpha W^\alpha_{\tilde{B}} \Phi_S \,, \tag{2.1}$$

where Φ_S is the superfield whose fermionic component is the singlino S. The Dirac bino mass is $M_{\tilde{B}} = c_i D/\Lambda_M$.

The global $U(1)_{R-L}$ symmetry, as all global symmetries, is broken due to gravity. Hence a Majorana mass for the bino is generated via anomaly mediation [15–17]

$$m_{\tilde{B}} = \frac{\beta(g_Y)}{g_Y} f_\phi \,, \tag{2.2}$$

where $\beta(g_Y)$ is the beta function for the hypercharge and F_ϕ is a conformal parameter satisfying

$$\frac{m_{3/2}^3}{16\pi^2 M_{\text{Pl}}^2} < f_\phi < m_{3/2} \,. \tag{2.3}$$

$m_{3/2}^2 = \sum(F_i^2 + D_i^2/2)/\sqrt{3}M_{Pl}^2$ is the gravitino mass. A Majorana mass for the singlino, m_S, is also expected to be produced, as well as Majorana masses for all other gauginos

and their Dirac partners. We assume the messenger scale Λ_M is below the Planck scale and $m_{\tilde{B}}, m_S \ll M_{\tilde{B}}$. In the following we use the term biνo to refer to the pseudo-Dirac fermion $\Psi_{\tilde{B}}^T = (\tilde{B}, S^\dagger)$ and its Weyl component $\tilde{B}$ interchangeably, which should be clear from the context. We use $M_{\tilde{B}}$ as the biνo mass, even though it gets small corrections from the Majorana masses as well.

It has been shown in [12] that the operators,[2]

$$\frac{f_i}{\Lambda_M^2} \int d^2\theta \, W'_\alpha W_{\tilde{B}}^\alpha H_u L_i \quad \text{and} \quad \frac{d_i}{\Lambda_M} \int d^4\theta \, \phi^\dagger \Phi_S H_u L_i \tag{2.4}$$

(where $\phi = 1 + \theta^2 m_{3/2}$) can generate two non-zero neutrino masses through the inverse seesaw mechanism [25, 26], with the bino-singlino pair acting as a pseudo-Dirac right-handed neutrino. Written in terms of their component fields, the neutrino-mass part of the Lagrangian becomes

$$\mathcal{L} \supset M_{\tilde{B}} \tilde{B} S + m_{\tilde{B}} \tilde{B}\tilde{B} + m_S \, SS + f_i \frac{M_{\tilde{B}}}{\Lambda_M} \ell_i h_u \tilde{B} + d_i \frac{m_{3/2}}{\Lambda_M} \ell_i h_u S \,, \tag{2.5}$$

where f_i and d_i, for $i = e, \mu, \tau$, are determined by neutrino mass differences as

$$f_i \simeq \begin{pmatrix} 0.35 \\ 0.85 \\ 0.35 \end{pmatrix}, \quad d_i \simeq \begin{pmatrix} -0.06 \\ 0.44 \\ 0.89 \end{pmatrix} \,. \tag{2.6}$$

After electroweak symmetry breaking the light neutrino masses are

$$m_1 = 0, \quad m_2 = \frac{m_{3/2} \, v^2}{\Lambda_M^2}(1 - \rho), \quad m_3 = \frac{m_{3/2} \, v^2}{\Lambda_M^2}(1 + \rho) \,, \tag{2.7}$$

where $\rho \simeq 0.7$ is determined by the neutrino mass splittings.

In the following we will study the current and future LHC constraints and forecasted constraints from future LLP experiments on the parameter space of this model. It will be shown that for a long-lived biνo which is observable at the LHC, the messenger scale needs to be high, up to 10^{11} TeV. This then requires a heavier gravitino than what was considered in earlier work. In figure 1 we show the gravitino mass as a function of Λ_M for normal hierarchy. (Inverted hierarchy is very similar.) For $\Lambda_M \gtrsim 10^5$ TeV, the gravitino needs to be heavier than $\sim$TeV in order to explain the neutrino masses.[3] The gravitino in this model decays primarily into photons and neutrinos with decay width $\Gamma_{3/2} \simeq \theta^2 m_{3/2}^3 / M_{\mathrm{Pl}}^2$, where $\theta \sim 10^{-3}$ is the neutrino-biνo mixing angle and $M_{\mathrm{Pl}} \simeq 1.2 \times 10^{16}$ TeV is the Planck mass. In figure 1 we also show the gravitino lifetime. In earlier work [13] it was mentioned that a gravitino with $O(10 \text{ keV})$ could be a dark matter candidate since it is stable within the lifetime of the universe. As the gravitino gets heavier, this decay width becomes larger. Above $m_{3/2} \sim O(10 \text{ GeV})$ the gravitino is no longer stable enough to constitute the dark

---

[2]These operators can be generated by integrating out two pairs of gauge singlets N_i, N'_i, with R-charge 1 and lepton number ∓ 1.

[3]In order to have both LHC-accessible squarks and a heavy gravitino, we imagine a scenario like [13] where there are two SUSY-breaking scales, with $\sqrt{D_1}, \sqrt{F_1} \sim 10$ TeV and $\sqrt{D_2}, \sqrt{F_2} \gtrsim 10^4$ TeV.
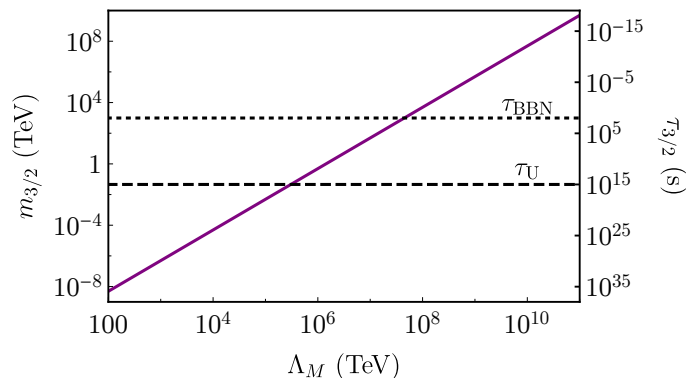
Figure 1. Gravitino mass required to explain neutrino masses as a function of messenger scale Λ_M for normal ordering. On the right y-axis we show the corresponding gravitino lifetime. The dashed horizontal line is the lifetime of the universe, τ_U, and the dotted line shows the time of BBN, τ_{BBN}, as reference points.

matter. If the gravitino decays around the time of Big Bang Nucleosynthesis (BBN), the produced photons could affect the production of light nuclei. In our model this could happen for $m_{3/2} \sim O(10^{1-3} \text{ TeV})$, corresponding to $\Lambda_M \sim 10^7 \text{ TeV}$. Note that there could also be new decay channels opening up if the gravitino is no longer the LSP, affecting the decay width. A detailed study of the gravitino is beyond the scope of this work. For now we ignore details of the gravitino behavior in this wide mass range and assume there are mechanisms, e.g. a low reheat temperature, to suppress the abundance of gravitinos with certain mass so that BBN proceeds as observed.

3 Biνo lifetime

The biνo decays primarily via its mixing with light neutrinos, with branching fraction $1/3$ to each channel: *(i)* $\tilde{B} \to W^- \ell^+$; *(ii)* $\tilde{B} \to Z\bar{\nu}$; and *(iii)* $\tilde{B} \to h\bar{\nu}$. Note that the decays to gravitinos is strongly suppressed by the Planck mass, $\Gamma(\tilde{B} \to \tilde{G}\gamma) \sim \frac{M_{\tilde{B}}^5}{M_{Pl}^2 m_{3/2}^2} \sim 10^{-8} \text{ eV}$, and the $\tilde{B} \to W^+ \ell^-$ decay is not allowed due to the $U(1)_{R-L}$ symmetry.

There are two interesting mass regimes for the biνo: *(i)* $M_{\tilde{B}} > M_{Z,W,h}$; and *(ii)* $M_{\tilde{B}} < M_{Z,W,h}$, which we will refer to as heavy and light biνo respectively. For simplicity we will consider $M_{\tilde{B}} > 125 \text{ GeV}$ and $M_{\tilde{B}} < 80 \text{ GeV}$ for each regime.

Heavy biνo. In this scenario the biνo can decay into on-shell W, Z, h final states via a 2-body process. The total decay width is

$$\Gamma_{\tilde{B}}^{\text{heavy}} \simeq \sum_{i=e,\mu,\tau} M_{\tilde{B}} Y_i^2 \simeq \frac{M_{\tilde{B}}^3}{\Lambda_M^2}, \quad \text{where } Y_i = f_i \frac{M_{\tilde{B}}}{\Lambda_M} . \tag{3.1}$$

Light biνo. In this regime, since the biνo is lighter than the gauge bosons, it has to decay through off-shell W, Z, h to 3-body final states.

$$\Gamma_{\tilde{B}}^{\text{light}} \simeq \sum_{i=e,\mu,\tau} \kappa Y_i^2 \frac{G_F^2 M_{\tilde{B}}^5}{192\pi^3} \simeq \kappa \frac{G_F^2 M_{\tilde{B}}^7}{192\pi^3 \Lambda_M^2}, \tag{3.2}$$

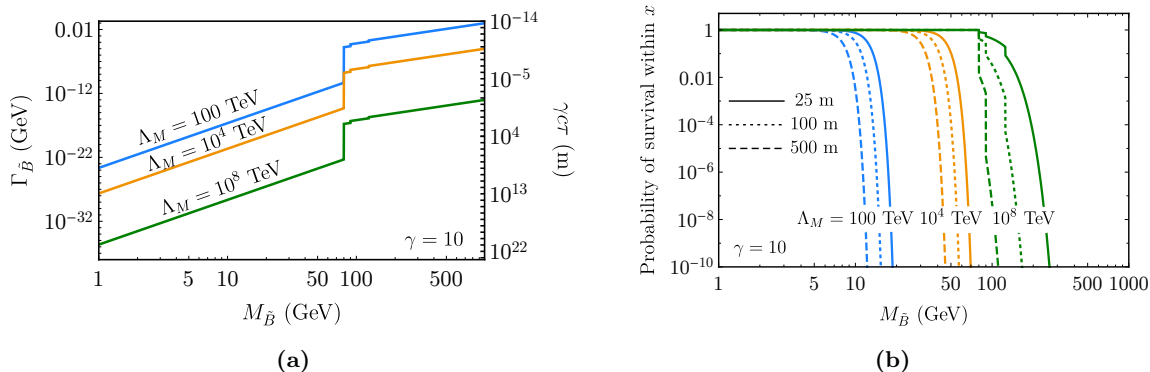**Figure 2.** *(a)* Biνo decay width and decay length versus the biνo mass $M_{\tilde{B}}$. We show three different choices of the messenger scale, $\Lambda_M = 10^2, 10^4, 10^8$ TeV. Below $M_{\tilde{B}} = 80$ GeV biνo decays to 3-body final states through off-shell gauge and Higgs bosons and hence the decay width is much smaller. *(b)* Probability of a biνo surviving, i.e. *not* having decayed, after traveling a distance $x = 25, 100, 500$ meters, roughly corresponding to the length of the ATLAS detector, and the distance between the biνo production point and MATHUSLA and FASER respectively. The Lorentz factor is taken to be $\gamma = 10$, which corresponds to a momentum of $\sim$ TeV for a 100 GeV biνo, as a benchmark value.

where κ is an $O(1)$ number which encodes phase-space integrals. For our analysis we will take $\kappa = 1$.

On the left panel in figure 2 we show the biνo lifetime for various messenger scales. It can be seen that the width drops several orders of magnitude below the $M_{\tilde{B}} \sim M_W$ threshold. On the same plot, we also give the decay length $\gamma c\tau$ of biνo assuming a benchmark boost factor of $\gamma = 10$, which shows the expected behavior where as the decay width gets smaller, the lifetime gets longer. It can be seen in this plot that for $\Lambda_M = 100$ TeV and $M_{\tilde{B}} > 100$ GeV, which was covered in [13], biνo decays within a nanometer of the production point. However for lighter biνo and larger messenger scale, biνo lifetime can be much longer.

For the long-lived particle searches, we are interested in how far the biνo travels before it decays. Interesting length scales are related to the size and placement of certain detectors. For example the ATLAS detector is ~ 25 meters in diameter while MATHUSLA is planned to be placed ~ 70 meters from CMS [3] and FASER is ~ 500 meters away from ATLAS interaction points [6]. The probability that a relativistic particle survives at a distance x away from its production point is

$$P(x) = \exp(-x/\gamma c\tau) \,, \tag{3.3}$$

where $\gamma = 1/\sqrt{1 - v^2/c^2}$ is the Lorentz factor and $\tau = 1/\Gamma$ is the lifetime of the particle at its rest frame. In the right panel of figure 2 we show the probability of survival of a biνo at various distances from the production point as a function of the biνo mass. For low messenger scales, e.g. for $\Lambda_M = 100$ TeV, the probability that the biνo will travel hundreds of meters is low for $M_{\tilde{B}} \gtrsim 10$ GeV. (Note that messenger scales below 100 TeV can be probed at the upcoming Mu2e experiment [12, 27] independent of the biνo mass.)

As the messenger scale gets larger, heavier biνos could survive longer distances with much higher probability.

The survival probability depends on the biνo momentum, in terms of the Lorentz factor γ. In this work we will be looking at biνo production from squark decays. Hence the energy and the velocity of the biνo depends on the squark energy and momentum as well as the biνo mass itself. Furthermore we will require the biνo to decay within a certain detector volume that is placed at a certain angle from the interaction point. Hence the numerical calculation of the probability factor is more involved. We describe the experiments we consider and our analysis in the next section.

4 Long-lived biνo at the LHC

In earlier work [13] the parameter space for a short-lived biνo — with proper decay length $c\tau \lesssim 100~\mu$m — was investigated. It has been found that current constraints go up to only $M_{\rm sq} \approx 950\,$GeV and squarks as light as $350\,$GeV are allowed for $M_{\tilde{B}} = 100 - 150\,$GeV. In the previous section we showed that biνo can be long lived if its mass is low and/or if the messenger scale is high. In this section we examine search strategies to look for a long-lived biνo at the LHC. Our results are shown in figure 4.

We assume a sparticle spectrum where first- and second-generation squarks are degenerate and third generation is decoupled. We assume sleptons, gluinos and charginos are also heavy and decoupled. The lightest neutralino is a pure biνo and the other neutralinos are heavier than the degenerate squarks. (See figure 1 of [13].) Depending on the gravitino mass, biνo is either the LSP or the NLSP. Due to the sparticle spectrum we assume, biνo is produced mainly through squark decays. After being produced the long-lived biνo decays into a combination of quarks, charged leptons and neutrinos. (See figure 3 for an example process.) Such an event gives two complimentary search possibilities at the LHC: (i) a long-lived biνo escapes the LHC as missing energy so that it can be searched for by the jets+$\not{E}_T$ searches; and (ii) biνo decays to charged leptons inside an LLP detector. There are several (proposed or recently being built) dedicated LLP detectors like MATHUSLA [1–3], FASER [4–6], and CODEX-b [7, 8]. Additionally, future ATLAS or CMS LLP searches can be sensitive to long-lived biνo decays [28, 29]. Here we will focus on the reach of proposed, dedicated LLP experiments.

4.1 Missing energy analysis

A long-lived biνo with $c\tau \gtrsim 100~\mu$m will leave the inner tracker system of ATLAS as missing energy such that missing energy searches can be used constrain the $M_{\rm sq} - M_{\tilde{B}}$ parameter space. The signature at the LHC is a 2j (from the biνo production) + $\not{E}_T$ final state for which we can recast the multijet+$\not{E}_T$ ATLAS analysis [30]. We implement our model in FEYNRULES [31] and generate 10K events with MADGRAPH5 [32], using PYTHIA8 [33] for parton shower and hadronization, and DELPHES [34] for detector simulation at $\sqrt{s} = 13\,$TeV and $\mathcal{L} = 36$ fb^{-1}. We use the default settings for jets in MADGRAPH5 with $R = 0.4$, $p_{Tj} > 20\,$GeV and $|\eta_j| < 5$. We generate signal events for biνos in the mass range $1\,$GeV $< M_{\tilde{B}} < M_{\rm sq}$ where we take first and second generation squarks to be

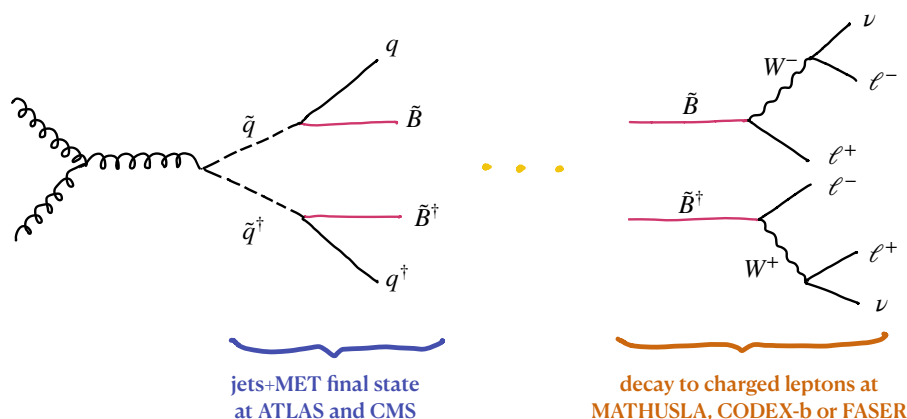**Figure 3.** An example process for biνo production via squark decays and subsequent decay of a long-lived biνo to charged leptons.
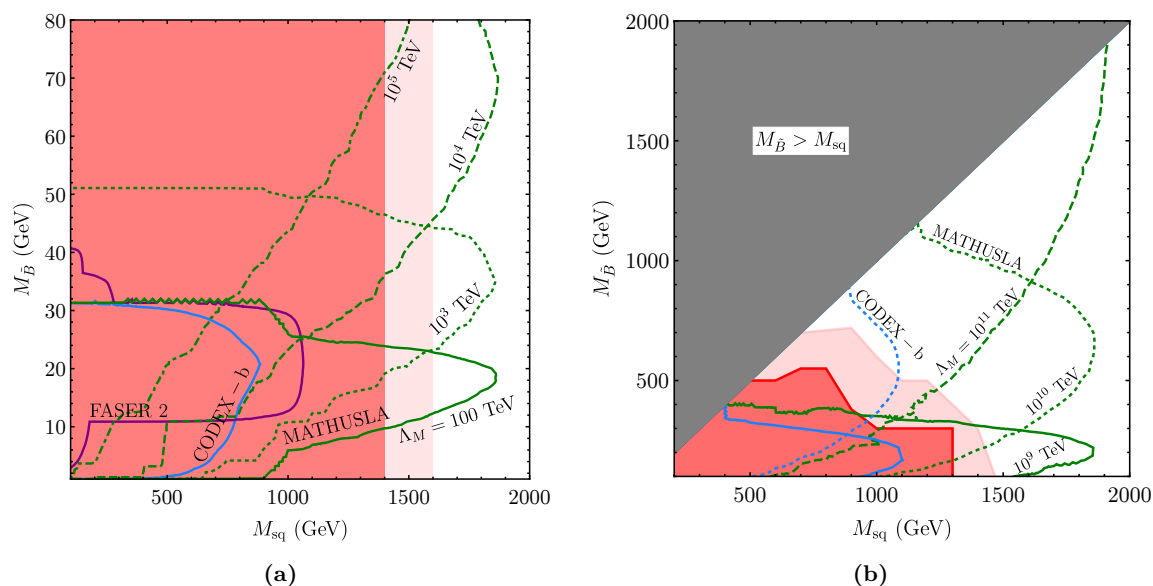
(a)   **(b)**

Figure 4. *(a)* Current and future constraints on light biνo mass region. Dark red shaded region shows the LHC constraint with $\mathcal{L} = 36\,\mathrm{fb}^{-1}$ of data while light pink is projection to $\mathcal{L} = 3\,\mathrm{ab}^{-1}$. The colored lines correspond to 5 events in each detector labeled with $\mathcal{L} = 3\,\mathrm{ab}^{-1}$. We show lines of different messenger scales, $\Lambda_M = 10^{2-5}$ TeV, for MATHUSLA. We show only $\Lambda_M = 100$ TeV for FASER 2 and CODEX-b because the parameter space that can be reached by these two experiments is already ruled out by ATLAS jets+$\not{E}_T$ search. *(b)* Current and future constraints on heavy biνo mass region. Dark red shaded region shows the LHC constraint with $\mathcal{L} = 36\,\mathrm{fb}^{-1}$ of data while light pink is projection to $\mathcal{L} = 3\,\mathrm{ab}^{-1}$. The green and blue colored lines correspond to 5 events in MATHUSLA and CODEX-b respectively with $\mathcal{L} = 3\,\mathrm{ab}^{-1}$. We show lines of different messenger scales, $\Lambda_M = 10^{9-11}$ TeV.

degenerate with mass $M_{\rm sq}$.[4] All other sparticle masses have been set to $10\,{\rm TeV}$ such that they are decoupled. We generated events with $10\,{\rm GeV}$ and $50\,{\rm GeV}$ intervals for $M_{\tilde{B}}$ and $M_{\rm sq}$ respectively and extrapolated our results for the intervening masses.

The $m_{\rm eff}$-based analysis by ATLAS [30] relies on the observable $m_{\rm eff}$ defined as the scalar sum of the transverse momenta of the leading jets and missing energy, $\not{E}_{\rm T}$. Taken together with $\not{E}_{\rm T}$, $m_{\rm eff}$ strongly suppresses the multijet background. There are 24 signal regions in this analysis. These regions are first divided according to jet multiplicities (2–6 jets). Signal regions with the same jet multiplicity are further divided according to the values of $m_{\rm eff}$ and the $\not{E}_{\rm T}/m_{\rm eff}$ or $\not{E}_{\rm T}/\sqrt{H_T}$ thresholds. In each signal region, different thresholds are applied on jet momenta and pseudorapidities to reduce the SM background. Cuts on the smallest azimuthal separation between $\not{E}_{\rm T}$ and the momenta of any of the reconstructed jets further reduce the multi-jet background. Two of the signal regions require two large radius jets and in all signal regions the required jet momentum $p_T > 50$ GeV and missing energy $\not{E}_{\rm T} > 250$ GeV. The thresholds on the observables which characterize the signal regions have been chosen to target models with squark or gluino pair production and direct decay of squarks/gluinos or one-step decay of squark/gluino via an intermediate chargino or neutralino. In order to identify the allowed parameter points we compare the signal cross-section to the measured cross-section limits at 95% C.L. in all 24 signal regions using the code from [35]. If the signal cross-section of a parameter point exceeds the measured cross-section at 95% C.L. in at least one bin we take this parameter point to be ruled out.

We also analyze the expected exclusion limits at the end of LHC Run 3 with $\sqrt{s} = 13$ TeV and $\mathcal{L} = 3$ ab^{-1}, by rescaling the expected number of signal and background events with luminosity. In order to obtain the allowed parameter region at a high-luminosity LHC we use the median expected exclusion significance [36][5]

$$
Z_{\rm exc} = \left[2 \left(s - b\log\left(\frac{b+s+x}{2b}\right) - \frac{b^2}{\Delta_b^2}\log\left(\frac{b-s+x}{2b}\right) \right) - (b+s-x)\left(1+\frac{b}{\Delta_b^2}\right) \right]^{1/2}, \quad (4.1)
$$

with

$$
x = \left[(s+b)^2 - 4sb\frac{\Delta_b^2}{(b+\Delta_b^2)} \right]^{1/2}, \quad (4.2)
$$

where s is the signal, b is background and Δ_b is the uncertainty on the background prediction. For a 95% C.L. median exclusion, we require $Z_{\rm exc} > 1.645$. We assume, as a conservative estimate, that the relative background uncertainty after 3 ab^{-1} remains the same as it is now, as presented in [30]. The estimate that Δ_b/b is constant could be improved upon, especially if the background is estimated from data in sidebands.

Our results are shown in figure 4 for $\sqrt{s} = 13$ TeV. We divide our analysis and results into low and high biνo mass regions. On the left panel of figure 4 we show the constraints

---

[4]We also looked at decoupling the second generation. In this case jets+$\not{E}_T$ constraints are milder due to the lowered production cross-section. However, expected number of biνo events at LLP detectors are also smaller due to the same cross-section suppression.

[5]See [37] for alternative expressions for the expected significance.

on the low biνo mass regime with $1\,\text{GeV} < M_{\tilde{B}} \lesssim 80\,\text{GeV}$. In this case the biνo is long lived even with $\Lambda_M = 100\,\text{TeV}$ and is seen as missing energy at ATLAS. In this parameter region squarks up to 1.4 TeV are excluded at $\mathcal{L} = 36\,\text{fb}^{-1}$, red/dark shaded area, and squark masses up to 1.6 TeV will be probed with $\mathcal{L} = 3\,\text{ab}^{-1}$, pink/light shaded area.[6] The constraints on the squark mass are independent of the biνo mass. On the right panel of figure 4 is the high biνo -mass region with $80\,\text{GeV} < M_{\tilde{B}} < M_{\text{sq}}$, where biνo is long lived. (Note that the exact messenger scale that corresponds to a long-lived biνo depends on $M_{\tilde{B}}$ and biνo energy. Generally it requires $\Lambda_M \gtrsim 10^4\,\text{TeV}$.) In this regime the constraints on the squark masses depend on the biνo mass. With $\mathcal{L} = 36\,\text{fb}^{-1}$, squark masses up to 1300 TeV are excluded for $M_{\tilde{B}} < 300\,\text{GeV}$. This limit can go up to 1450 GeV with $\mathcal{L} = 3\,\text{ab}^{-1}$.[7] On the other hand, squarks as light as 600 GeV are still allowed for heavier biνo.

4.2 LLP detectors

In this section we study the cases where the biνo decays inside one of the LLP detectors, namely MATHUSLA, CODEX-b and FASER. The parameter space for such decays depends on the biνo mass and the messenger scale, as can be observed in figure 2. For this analysis we follow [38], in which the required steps were very clearly laid out.

The number of biνo events that can be observed in a detector D = MATHUSLA, FASER or CODEX-b is

$$N_{\tilde{B}}^{D} = \mathcal{L} \times \sigma_{\tilde{B}} \times Br \times P(\tilde{B} \in D)\,, \tag{4.3}$$

where $\sigma_{\tilde{B}}$ is the biνo production cross-section at the LHC at $\sqrt{s} = 13\,\text{TeV}$ and $Br \simeq 0.7$ is the branching fraction of biνo to charged leptons [13]. We give our results for $\mathcal{L} = 3\,\text{ab}^{-1}$ for MATHUSLA and FASER, but only $300\,\text{fb}^{-1}$ for CODEX-b since LHCb receives a tenth of the luminosity of CMS and ATLAS.

$P(\tilde{B} \in D)$ captures the decay probability of biνo inside the detector and needs to be calculated for each detector geometry. (See section III of [38] for details.) In order to find this quantity we generate 10K parton level $gg \to q\bar{q}\tilde{B}\tilde{B}^{\dagger}$ events with MADGRAPH5 for each squark and biνo mass point described in the previous section. We analyze the results in MATHEMATICA with a routine written by D. Curtin [39]. The probability that a biνo particle with certain momentum will decay inside a detector depends on where the detector is and the detector geometry. Without going into too much detail, the necessary information about each detector can be summarized as follows.

- *MATHUSLA* [1–3] is a proposed experiment that will be 60 m in horizontal and 68 m in vertical distance from the CMS interaction point. Its size will be $100\,\text{m} \times 25\,\text{m} \times 25\,\text{m}$.

- *CODEX-b* [7, 8] is proposed to be 25 m from LHCb interaction point. It will be a cube of 10 m × 10 m × 10 m.

---

[6]For decoupled second generation, the current constraint is 1.2 TeV and future reach will 1.4 TeV.

[7]Corresponding current and future constraints for a decoupled second generation scenario is $M_{\text{sq}} = 1\,\text{TeV}$ and 1.2 TeV respectively.

- *FASER* [4–6] is being built 470 m from ATLAS inside the LHC tunnel. In its first version it is a cylinder with 10 cm radius and 1.5 m length. It is planned to be upgraded to a radius of 1 m and length of 5 m in the next LHC upgrade. We forecast our results for FASER 2, the upgraded version, to show that even this larger version will not be able to probe the parameter space we study.

In figure 4 we show contours of five charged lepton events at each detector for $\mathcal{L} = 3 \text{ ab}^{-1}$. For low mass bi$\nu$o (left panel in figure 4) the parameter space relevant for FASER and CODEX-b is completely ruled out by current ATLAS jets+$\not{E}_T$ searches. For this mass region MATHUSLA can still be complementary to and even competitive against future ATLAS missing energy searches for a messenger scale up to $\sim 10^4$ TeV. For heavier biνo (right panel in figure 4), with mass larger than ~ 100 GeV, the messenger scale that can be probed is higher. In this regime MATHUSLA will be able to detect events for 10^9 TeV $\lesssim \Lambda_M \lesssim 10^{11}$ TeV with 3 ab^{-1} luminosity. Most importantly, the squark mass that can be probed by MATHUSLA is much higher, ~ 1.9 TeV, than what will be probed by jets+$\not{E}_T$ searches. Even though it suffers from the lowered luminosity at LHCb, CODEX-b still shows some reach for the heavy biνo regime, for lower squark mass, $M_{\text{sq}} \sim 1$ TeV and heavy biνo, $M_{\tilde{B}} > 600$ GeV. It is also worth noting that missing energy searches can only put a lower limit on Λ_M while MATHUSLA and CODEX-b can target specific values of both biνo mass and the messenger scale.

Having relied on the clean and clear LLP analysis prescription described in [38], we also briefly describe the differences of the two works. In [38] the authors study an R-parity-violating MSSM scenario with the term $\lambda'_{ijk} L_i Q_j D^c_k$ and look at a scenario where the lightest neutralino is produced in meson decays and decays into lighter mesons and charged leptons via this term. In the model we study, the λ' term is not allowed due to the U(1)$_{R-L}$ symmetry. It is expected to be generated when U(1)$_{R-L}$ is broken, but its size is suppressed by $m_{3/2}/\Lambda_M$ compared to the U(1)$_{R-L}$-symmetric terms we investigate.

5 Summary & conclusions

In this work we studied a model which presents an LLP, namely the biνo, which is directly related to the explanation of neutrino masses. In [12] it was shown that in a U(1)$_{R-L}$-symmetric supersymmetric model the observed neutrino mass spectrum can be achieved via an inverse seesaw mechanism, in which the role of right-handed neutrinos is played by the pseudo-Dirac biνo. The lifetime of the biνo depends on its mass and the messenger scale. The smaller the biνo mass and/or the larger the messenger scale the longer lived is the biνo. Hence probing the biνo lifetime in this scenario can lead to insights not only on the SUSY spectrum but also on SUSY breaking. If the biνo is long-lived, it escapes ATLAS or CMS as missing energy and depending on the biνo mass, biνo momentum and the messenger scale, it potentially decays inside dedicated LLP experiments like FASER, CODEX-b, or MATHUSLA.

In order to study the potential of the LLP experiments, we first recast the most recent jets+$\not{E}_T$ searches from ATLAS, using $\sqrt{s} = 13$ TeV and $\mathcal{L} = 36$ fb^{-1} to obtain

the currently allowed parameter space. Then we simulated the reach of these experiment assuming a luminosity of $\mathcal{L} = 3\text{ ab}^{-1}$. Our results are summarized in figure 4. We considered two regimes for the biνo mass. **(i)** A light biνo, with mass below the W boson mass, decays through off-shell weak gauge or the Higgs bosons to a 3-body final state. In this case the current constraints from jets+$\not{E}_T$ searches exclude squark masses below 1.4 TeV independent of the biνo mass for $\Lambda_M \gtrsim O(10\text{ TeV})$. We then look at the reach of dedicated LLP detectors for this mass regime for $\Lambda_M > 100\text{ TeV}$. We see that FASER and CODEX-b are not competitive in this scenario, both of which can only cover a low squark-mass region which is already excluded by jets+$\not{E}_T$ searches. However MATHUSLA is sensitive to messenger scales between $100 - 10^5$ TeV, part of which will not be covered by jets+$\not{E}_T$ searches at $\mathcal{L} = 3\text{ ab}^{-1}$. **(ii)** For heavy bi$\nu$os with mass above the Higgs mass the decay channel is into on-shell weak gauge bosons or the Higgs boson. In this regime the decay width is larger and current jets+$\not{E}_T$ constraints exclude biνo masses below 500 GeV for squark masses below 1.3 TeV. In this regime MATHUSLA again has the best reach amongst the proposed LLP detectors. It can probe biνo and squark masses up to 2 TeV for messenger scales between $10^9 - 10^{11}$ TeV. CODEX-b also becomes more competitive compared to the low biνo-mass regime.

Another possibility to search for a long-lived biνo in this model is to search for displaced vertices in ATLAS or CMS. Recent analysis which rely on prompt jets and a displaced dilepton vertex [40] have shown that such analyses are possible with low background rates. The signature in our model scenario are two prompt jets and a displaced vertex with a combination of jets, charged leptons and missing energy. One significant difference between our model and generic RPV MSSM models this analysis relied on is that the charged leptons in the biνo decays does not point to a vertex, see, e.g., figure 3. In the absence of a public analysis, we will leave the study of displaced vertices inside LHC detectors in our model for future work.

In our previous analysis on short-lived biνos [13], we focused on a messenger scale of 100 TeV and biνo masses between 100 GeV-1 TeV. In this current work we extended that parameter region to a biνo mass of 1 GeV as well as much higher messenger scales, up to 10^{11} TeV. Together, we have analyzed a vast region of parameter space in this model.

Acknowledgments

References

[1] J.P. Chou, D. Curtin and H.J. Lubatti, *New Detectors to Explore the Lifetime Frontier*, *Phys. Lett. B* **767** (2017) 29 [arXiv:1606.06298] [ɪɴSPIRE].

[2] MATHUSLA collaboration, *A Letter of Intent for MATHUSLA: A Dedicated Displaced Vertex Detector above ATLAS or CMS.*, arXiv:1811.00927 [ɪɴSPIRE].

[3] MATHUSLA collaboration, *An Update to the Letter of Intent for MATHUSLA: Search for Long-Lived Particles at the HL-LHC*, arXiv:2009.01693 [ɪɴSPIRE].

[4] J.L. Feng, I. Galon, F. Kling and S. Trojanowski, *ForwArd Search ExpeRiment at the LHC*, *Phys. Rev. D* **97** (2018) 035001 [arXiv:1708.09389] [ɪɴSPIRE].

[5] FASER collaboration, *Letter of Intent for FASER: ForwArd Search ExpeRiment at the LHC*, arXiv:1811.10243 [ɪɴSPIRE].

[6] FASER collaboration, *FASER: ForwArd Search ExpeRiment at the LHC*, arXiv:1901.04468 [ɪɴSPIRE].

[7] V.V. Gligorov, S. Knapen, M. Papucci and D.J. Robinson, *Searching for Long-lived Particles: A Compact Detector for Exotics at LHCb*, *Phys. Rev. D* **97** (2018) 015023 [arXiv:1708.09395] [ɪɴSPIRE].

[8] G. Aielli et al., *Expression of interest for the CODEX-b detector*, *Eur. Phys. J. C* **80** (2020) 1177 [arXiv:1911.00481] [ɪɴSPIRE].

[9] V.V. Gligorov, S. Knapen, B. Nachman, M. Papucci and D.J. Robinson, *Leveraging the ALICE/L3 cavern for long-lived particle searches*, *Phys. Rev. D* **99** (2019) 015023 [arXiv:1810.03636] [ɪɴSPIRE].

[10] J. Alimena et al., *Searching for long-lived particles beyond the Standard Model at the Large Hadron Collider*, *J. Phys. G* **47** (2020) 090501 [arXiv:1903.04497] [ɪɴSPIRE].

[11] L. Lee, C. Ohm, A. Soffer and T.-T. Yu, *Collider Searches for Long-Lived Particles Beyond the Standard Model*, *Prog. Part. Nucl. Phys.* **106** (2019) 210 [arXiv:1810.12602] [ɪɴSPIRE].

[12] P. Coloma and S. Ipek, *Neutrino masses from a pseudo-Dirac Bino*, *Phys. Rev. Lett.* **117** (2016) 111803 [arXiv:1606.06372] [ɪɴSPIRE].

[13] J. Gehrlein, S. Ipek and P.J. Fox, *Biνo Phenomenology at the LHC*, *JHEP* **03** (2019) 073 [arXiv:1901.09284] [ɪɴSPIRE].

[14] L.J. Hall and L. Randall, *U(1)-R symmetric supersymmetry*, *Nucl. Phys. B* **352** (1991) 289 [ɪɴSPIRE].

[15] L. Randall and R. Sundrum, *Out of this world supersymmetry breaking*, *Nucl. Phys. B* **557** (1999) 79 [hep-th/9810155] [ɪɴSPIRE].

[16] G.F. Giudice, M.A. Luty, H. Murayama and R. Rattazzi, *Gaugino mass without singlets*, *JHEP* **12** (1998) 027 [hep-ph/9810442] [ɪɴSPIRE].

[17] N. Arkani-Hamed, S. Dimopoulos, G.F. Giudice and A. Romanino, *Aspects of split supersymmetry*, *Nucl. Phys. B* **709** (2005) 3 [hep-ph/0409232] [ɪɴSPIRE].

[18] P. Fayet, *Supergauge Invariant Extension of the Higgs Mechanism and a Model for the electron and Its Neutrino*, *Nucl. Phys. B* **90** (1975) 104 [ɪɴSPIRE].

[19] P. Fayet, *Fermi-Bose Hypersymmetry*, *Nucl. Phys. B* **113** (1976) 135 [ɪɴSPIRE].

[20] C. Frugiuele, T. Gregoire, P. Kumar and E. Ponton, $''L = R''$ − U(1)$_R$ *Lepton Number at the LHC*, *JHEP* **05** (2013) 012 [arXiv:1210.5257] [INSPIRE].

[21] C. Alvarado, A. Delgado and A. Martin, *Constraining the R-symmetric chargino NLSP at the LHC*, *Phys. Rev. D* **97** (2018) 115044 [arXiv:1803.00624] [INSPIRE].

[22] P. Diessner, W. Kotlarski, S. Liebschner and D. Stöckinger, *Squark production in R-symmetric SUSY with Dirac gluinos: NLO corrections*, *JHEP* **10** (2017) 142 [arXiv:1707.04557] [INSPIRE].

[23] J. Kalinowski, *SUSY with R-symmetry: confronting EW precision observables and LHC constraints*, *Acta Phys. Polon. B* **47** (2016) 203 [arXiv:1510.06652] [INSPIRE].

[24] P.J. Fox, A.E. Nelson and N. Weiner, *Dirac gaugino masses and supersoft supersymmetry breaking*, *JHEP* **08** (2002) 035 [hep-ph/0206096] [INSPIRE].

[25] R.N. Mohapatra, *Mechanism for Understanding Small Neutrino Mass in Superstring Theories*, *Phys. Rev. Lett.* **56** (1986) 561 [INSPIRE].

[26] R.N. Mohapatra and J.W.F. Valle, *Neutrino Mass and Baryon Number Nonconservation in Superstring Models*, *Phys. Rev. D***34** (1986) 1642 [INSPIRE].

[27] MU2E collaboration, *Mu2e Technical Design Report*, arXiv:1501.05241 [INSPIRE].

[28] ATLAS collaborations, *Performance of vertex reconstruction algorithms for detection of new long-lived particle decays within the ATLAS inner detector*, CERN, Geneva, Switzerland (2019) ATL-PHYS-PUB-2019-013.

[29] ATLAS collaborations, *Sensitivity of the ATLAS experiment to long-lived particles with a displaced vertex and E_T^{miss} signature at the HL-LHC*, CERN, Geneva, Switzerland (2018) ATL-PHYS-PUB-2018-033.

[30] ATLAS collaborations, *Search for squarks and gluinos in final states with jets and missing transverse momentum using 36 fb^{-1} of $\sqrt{s} = 13$ TeV pp collision data with the ATLAS detector*, CERN, Geneva, Switzerland (2017) ATLAS-CONF-2017-022.

[31] A. Alloul, N.D. Christensen, C. Degrande, C. Duhr and B. Fuks, *FeynRules 2.0 - A complete toolbox for tree-level phenomenology*, *Comput. Phys. Commun.* **185** (2014) 2250 [arXiv:1310.1921] [INSPIRE].

[32] J. Alwall, R. Frederix, S. Frixione, V. Hirschi, F. Maltoni, O. Mattelaer et al., *The automated computation of tree-level and next-to-leading order differential cross sections, and their matching to parton shower simulations*, *JHEP* **07** (2014) 079 [arXiv:1405.0301] [INSPIRE].

[33] T. Sjöstrand, S. Ask, J.R. Christiansen, R. Corke, N. Desai, P. Ilten et al., *An introduction to PYTHIA 8.2*, *Comput. Phys. Commun.* **191** (2015) 159 [arXiv:1410.3012] [INSPIRE].

[34] DELPHES 3 collaboration, *DELPHES 3, A modular framework for fast simulation of a generic collider experiment*, *JHEP* **02** (2014) 057 [arXiv:1307.6346] [INSPIRE].

[35] P. Asadi, M.R. Buckley, A. DiFranzo, A. Monteux and D. Shih, *Digging Deeper for New Physics in the LHC Data*, *JHEP* **11** (2017) 194 [arXiv:1707.05783] [INSPIRE].

[36] N. Kumar and S.P. Martin, *Vectorlike Leptons at the Large Hadron Collider*, *Phys. Rev. D* **92** (2015) 115018 [arXiv:1510.03456] [INSPIRE].

[37] P.N. Bhattiprolu, S.P. Martin and J.D. Wells, *Criteria for projected discovery and exclusion sensitivities of counting experiments*, *Eur. Phys. J. C* **81** (2021) 123 [arXiv:2009.07249] [INSPIRE].

[38] D. Dercks, J. De Vries, H.K. Dreiner and Z.S. Wang, *R-parity Violation and Light Neutralinos at CODEX-b, FASER, and MATHUSLA*, *Phys. Rev. D* **99** (2019) 055039 [arXiv:1810.03617] [INSPIRE].

[39] D. Curtin, *CFHEP Monte Carlo Tutorial*, http://insti.physics.sunysb.edu/~curtin/ CFHEP_tutorial/MadEvent_analysis_CFHEPtut.nb.

[40] ATLAS collaboration, *Search for displaced vertices of oppositely charged leptons from decays of long-lived particles in pp collisions at $\sqrt{s} = 13$ TeV with the ATLAS detector*, *Phys. Lett. B* **801** (2020) 135114 [arXiv:1907.10037] [INSPIRE].